

#### **OPEN ACCESS**

EDITED BY Fabrizio Carta, University of Florence, Italy

REVIEWED BY
Meng Fu,
University of Science and Technology of China
(USTC), China
Hesong Wang,
Fourth Hospital of Hebei Medical University,

\*CORRESPONDENCE
Xiufeng Li

☑ lixiufengsci@163.com

RECEIVED 12 July 2025
REVISED 20 October 2025
ACCEPTED 07 November 2025
PUBLISHED 26 November 2025

#### CITATION

Zhang Y, Zhang H and Li X (2025) Case Report: Two cases of non-small cell lung cancer with coexistence of *NTRK2* fusion and *EGFR* mutations. *Front. Oncol.* 15:1664782.

Front. Oncol. 15:1664782. doi: 10.3389/fonc.2025.1664782

#### COPYRIGHT

© 2025 Zhang, Zhang and Li. This is an openaccess article distributed under the terms of the Creative Commons Attribution License (CC BY). The use, distribution or reproduction in other forums is permitted, provided the original author(s) and the copyright owner(s) are credited and that the original publication in this journal is cited, in accordance with accepted academic practice. No use, distribution or reproduction is permitted which does not comply with these terms.

# Case Report: Two cases of non-small cell lung cancer with coexistence of *NTRK2* fusion and *EGFR* mutations

Yuping Zhang, Hengming Zhang and Xiufeng Li\*

Precision Pathology Diagnosis Center, Weifang People's Hospital, Shandong Second Medical University, Weifang, China

**Objective:** To investigate the clinical and pathological characteristics of patients with non-small cell lung cancer exhibiting coexistence of *NTRK2* fusion and *EGFR* mutations.

**Methods:** Clinical data, as well as histopathological, immunohistochemical, and molecular pathological characteristics, of two patients harboring both *NTRK2* gene fusions and *EGFR* gene mutations were retrospectively analyzed, and relevant literature was also reviewed.

**Results:** Both patients were women aged 57 and 66 years. The two cases were diagnosed as invasive lung adenocarcinoma, and immunohistochemical staining showed that all tumor cells expressed CK7, Napsin A, TTF-1, and PD-L1. In Case 1, an *EGFR* mutation in the primary lung lesion, coexistence of *NTRK2* fusion and *EGFR* mutation in liver metastases, and concurrent *MET* gene amplification and *FGFR1* gene mutation were observed. In Case 2, the coexistence of *NTRK2* fusion and *EGFR* mutation was detected in the primary lung lesion. The Tumor Mutation Burden (TMB) and microsatellite status were classified as TMB-L and MicroSatellite Stable (MSS), respectively, in both cases. Case 1 received osimertinib combined with savolitinib, had 33 months of follow-up, and achieved a partial response. Case 2 received furmonertinib and achieved a complete response.

**Conclusion:** *NTRK2* fusion coexisting with *EGFR* mutations is a rare molecular characteristic of non-small cell lung cancer, accompanied by positive PD-L1 expression, and may serve as a promising biomarker for targeted therapy.

KEYWORDS

non-small cell lung cancer, molecular testing, NTRK2, EGFR, fusion and mutation

#### 1 Introduction

Currently, the survival outcomes of patients with non-small cell lung cancer (NSCLC) can be significantly improved through precise molecular typing, attributable to advancements in chemotherapy, targeted therapy, and immunotherapy. Notably, the molecular variation spectrum of patients with NSCLC in China differs from that of the Western population, especially for adenocarcinoma (1, 2). With the development of in-depth discovery

technologies and exploration of targeted molecules and tumor-related pathways, an increasing number of genes and loci related to NSCLC treatment have been identified. Multiple variations in targeted therapy-related genes have been discovered, including common variations in genes, such as EGFR, KRAS, and ALK; minority mutations in genes, such as ROS1, MET, HER2, BRAF, and RET; and rare mutations in genes, such as NTRK and NRG1/2. In the same case, many variations generally occur exclusively, and the coexistence of these two types of variations has been reported in only a very small number of cases, such as EGFR mutations coexisting with variations in ALK, HER2, RET, and ROS1 genes (3, 4). Recently, the coexistence of these genetic alterations has been increasingly observed—for example, EGFR mutations coexisting with NTRK1 translocations in NSCLC (5). Here, the clinical, histopathological, and molecular pathological characteristics, targeted therapy, and prognosis of two patients with NSCLC exhibiting coexistence of NTRK2 fusion and EGFR mutations are presented to enhance understanding of such rare gene covariations and provide a basis for precise targeted therapy in NSCLC.

## 2 Case description

#### 2.1 Case information

Both patients were diagnosed with invasive lung adenocarcinoma at the Precision Case Diagnosis Center of Weifang People's Hospital. All histopathological diagnoses were reviewed by two senior pathologists. Baseline patient characteristics were collected, including age, sex, clinical manifestations, lymph node and/or distant metastases, imaging findings, pathological examinations (histopathological and molecular tests), treatment, and follow-up information.

#### 2.2 Methods

# 2.2.1 Hematoxylin and eosin and immunohistochemical staining

Specimens from the two cases were fixed in 10% neutral formalin solution, paraffin-embedded, sectioned into 3-µm-thick slices, and processed for hematoxylin and eosin staining and immunohistochemical analysis following the manufacturer's instructions. An immunohistochemical assay for PD-L1 detection was performed using the Dako Autostainer Link 48 instrument (Agilent Technologies, Singapore Pte. Ltd., Roche Diagnostic Products Co., Ltd, Shanghai, China), and other primary antibodies-including ALK [D5F3, Roche Diagnostics Products (Shanghai) Co., Ltd., Zhongshan Golden Bridge Biotechnology Co. Ltd Co., Ltd, Beijing, China], CK7, Napsin A, TTF-1, P40, CK5/6, CK20, HepPar-1, CK19, CK8/18, Glypican-3, and Ki-67 (ZSGB-BIO Co. Ltd., Beijing, China)—were analyzed using the Roche BENCHMARK XT automated immunohistochemical instrument (Roche Ventana, Roche Diagnostic Products Co., Ltd, Shanghai, China).

#### 2.2.2 Fluorescence in situ hybridization assay

*NTRK2* rearrangement was detected using a fluorescence *in situ* hybridization (FISH) assay following the manufacturer's instructions. The *NTRK2* probe was purchased from Wuhan Kanglu Biotechnology Co., Ltd., HealthCare Biotechnology Co., Ltd, Wuhan, China. Red and green signals were considered separated when the distance between them exceeded the sum of their diameters in tumor cell nuclei, and a separation ratio  $\geq 15\%$  was recognized as positive (separation ratio = number of positive cells/number of total cells  $\times$  100%).

#### 2.2.3 Next-generation sequencing

DNA was extracted using a magnetic bead-based FFPE DNA extraction kit (Guangzhou Meiji Biotechnology Co., Ltd., Majorbio Biotechnology Co., Ltd., Shanghai, China). The concentration and quality of DNA were assessed using a NanoDrop 2000 and Qubit 4.0, respectively. DNA sequencing was performed using a targeted high-throughput next-generation sequencing panel for NSCLC [Yuanma Gene Technology (Suzhou) Co., Ltd., MetaGene Technology Co., Ltd, Suzhou, China; National Medical Device Registration No. 20213400525]. TMB and Microsatellite instability (MSI) were detected using the Non-Small Cell Lung Cancer Tissue TMB Detection Kit (Nanjing ShiHe Medical Devices Co., Ltd., Shihejiyin Technology Co., Ltd, Nanjing, China).

# 3 Diagnostic assessment

#### 3.1 Clinical features

Both cases involved women.

Patient 1, aged 59 years, was diagnosed at our hospital on October 26, 2022, and presented with an unexplained headache, predominantly generalized cranial distending pain. Plain and contrast-enhanced computed tomography (CT) and cranial magnetic resonance imaging (MRI) showed a solid nodule in the left upper lung lobe with mediastinal lymphadenopathy, multiple ground-glass nodules in both lungs, and multiple intracranial spaceoccupying lesions. The patient was diagnosed with lung cancer accompanied by brain metastasis (Figures 1A, B). No positive signs were found during physical examination. Blood routine test revealed white blood cell count  $6.86 \times 10^9$ /L (normal range:  $3.5-9.5 \times 10^9$ /L), red blood cell count  $3.69 \times 10^{12}/L$  (normal range:  $3.8-5.1 \times 10^{12}/L$ ), hemoglobin 113 g/L (normal range: 115–150 g/L), and platelets 232  $\times$  $10^9/L$  (normal range:  $125-350 \times 10^9/L$ ). Blood biochemical test revealed total protein 56.5 g/L (normal range: 65-85 g/L), albumin 35.4 g/L (normal range: 40-55 g/L), and urea 2.2 mmol/L (normal range: 2.6-7.5 mmol/L); alanine aminotransferase, aspartate aminotransferase, alkaline phosphatase, glucose, and creatinine were all normal. Tumor markers in blood tests were within normal ranges, including alpha-fetoprotein, carcinoembryonic antigen (CEA), carbohydrate antigen 19-9, and carbohydrate antigen 125. Because of intermittent liver pain, an enhanced CT examination of the chest and abdomen was performed in September 2024 (Figures 1C, D), revealing metastases in the liver and left adrenal gland. In November

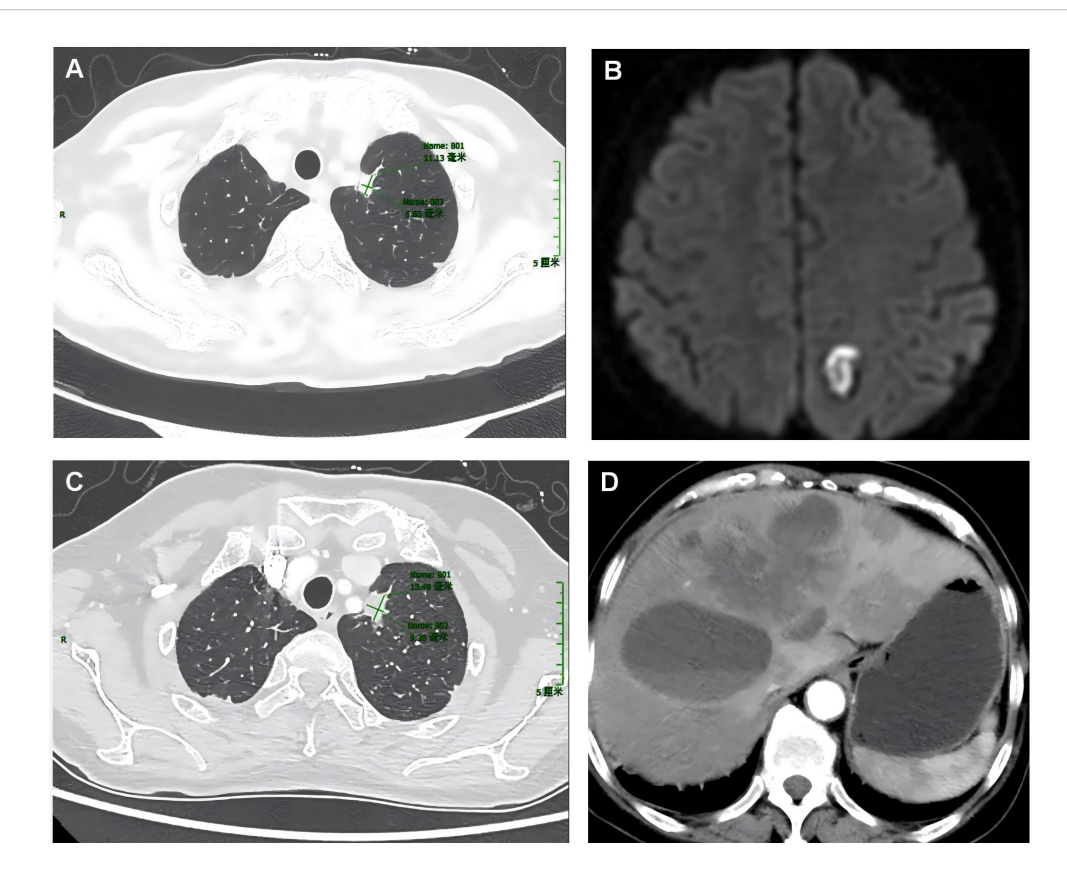


FIGURE 1
Plain computed tomography (CT) images of the lung and liver lesions, as well as the cranial magnetic resonance images of the first patient. The plain CT scan upon admission showed a mass in the lungs (A), whereas the magnetic resonance imaging of the brain indicated brain metastases (B). In September 2024, plain CT scans of the chest and liver showed lung lesions (C) and liver metastases (D).

2024, tumor markers in blood were elevated, including CYFRA21-1 (cytokeratin 19 fragment, 13.86 ng/mL, normal value: 0–3.3 ng/mL), neuron-specific enolase (21.81 ng/mL, normal value: 0–16.3 ng/mL), and CEA (28.81 ng/mL, normal value: 0–5 ng/mL).

Patient 2 was 66 years old. Owing to unexplained coughing and expectoration with a small amount of white, sticky, or yellow phlegm that was difficult to expel, a CT examination was performed at a local hospital. The results demonstrated space-occupying lesions and multiple nodular foci in both lungs. Traditional Chinese medicine treatment was administered, but no improvement was observed. The patient visited our hospital in October 2024. Enhanced chest CT (Figure 2) showed a soft-tissue-density mass in the lower lobe of the right lung, 35 mm × 26 mm in size, irregular in shape, with spicules and pleural traction visible at the margin, and moderate enhancement on the contrast scan. No positive signs were found during physical examination. Routine blood tests showed normal white blood cell count, red blood cell count, hemoglobin, platelet count, and normal biochemical results for alanine aminotransferase, aspartate aminotransferase, alkaline phosphatase, glucose, creatinine, urea, total protein, and albumin. Elevated tumor marker levels were observed in blood, including CYFRA21-1 (4.26 ng/mL, normal value: 0-3.3 ng/mL), neuron-specific enolase (25.84 ng/mL, normal value: 0-16.3 ng/mL), and CEA (41.83 ng/mL, normal value: 0-5 ng/mL).

Patient 1 had no history of other health issues. Patient 2 had a 10-year history of chronic bronchitis but did not receive regular treatment. None of the patients had a history of hypertension, diabetes, cardiovascular or cerebrovascular diseases, or infectious diseases, such as hepatitis or tuberculosis, nor had they been in close contact with such cases. Both patients had no history of drug or food allergies; no unhealthy habits, such as smoking, drinking, or drug abuse; no history of trauma, surgery, or blood transfusion; and no family genetic history.

#### 3.2 Pathological features

The morphology of the lung lesion biopsy tissue in Patient 1 in November 2022 is shown in Figure 3. The tumor was partially acinar and slightly papillary, with cells of varying sizes, abundant eosinophilic cytoplasm, and rare mitotic figures (Supplementary Figures S1A, B). Immunohistochemical staining was positive for CK7, Napsin A, and TTF-1; negative for CK5/6 and P40; and 8% positive for Ki-67. Therefore, the patient was diagnosed with invasive lung adenocarcinoma.

The morphology of the liver metastases in Patient 1 in December 2024 is shown in Figure 4. Atypical cells were observed

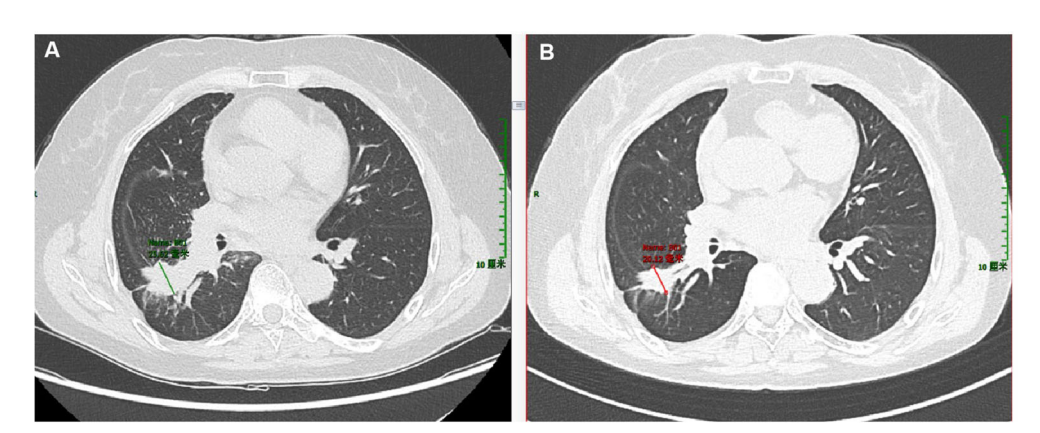


FIGURE 2
Enhanced computed tomography (CT) images of the lungs of the second patient. (A) CT scan of the lungs taken upon admission in April 2024. (B) CT scan of the lungs re-performed in November 2024.

in proliferating fibrous tissue with marked cellular atypia (Figures 3A, B). Immunohistochemical staining was positive for CK7 (Figure 3C), TTF-1 (Figure 3D), Napsin A (Figure 3E), CK19, and CK8/18; weakly positive for CK20; scattered positive for P40; partially weakly positive for Glypican-3; and negative for HepPar-1 (Figure 3F). The Ki-67 positivity index was 85%. The PD-L1 (22C3) combined positive score was 50, calculated as follows: (number of PD-L1-positive tumor-associated immune cells)/total number of viable tumor cells × 100. The ALK (D5F3) companion diagnostic test was negative (tumor cells, positive control + negative control). The patient was diagnosed with lung adenocarcinoma with liver metastasis.

Microscopic observation of the lung lesion puncture tissue in Patient 2 (Supplementary Figures S2A, B) showed that the tumor was located beneath the hyperplastic fibers and bronchial mucosa, with tumor cells of varying sizes, abundant cytoplasm, eosinophilia, and rare mitotic figures. Further immunohistochemical staining was positive for CK7 (Supplementary Figure S2C) and TTF-1 (Supplementary Figure S2D) and negative for CK5/6 (Supplementary Figure S2E) and P40 (Supplementary Figure S2F). The Ki-67 index was 10%. The PD-L1 (22C3) Tumor Proportion Score (TPS) (%) was 2%, which was calculated as the number of PD-L1 staining-positive tumor cells/total number of viable tumor cells × 100%. The ALK (D5F3) companion diagnosis was negative (tumor cells, positive control + negative control). Ultimately, the patient was diagnosed with invasive lung adenocarcinoma.

In differential diagnosis, pulmonary invasive adenocarcinoma should be differentiated from squamous cell carcinoma and small-cell carcinoma of the lungs. Morphologically, adenocarcinoma typically presents as glandular, sheet-like, and papillary growth; squamous cell carcinoma shows nest-like and sheet-like growth with keratinization and cell bridges visible; small-cell carcinoma presents as sheet-like and nest-like growth with organ-like or compression arrangement, rich blood vessels, small cells, and chromatin in a salt-and-pepper pattern. Regarding immunohistochemical expression, adenocarcinoma expresses CK7, TTF-1, and Napsin A; squamous cell carcinoma expresses P40 and CK5/6; and small-cell carcinoma expresses CK broad (with focal positivity at the nuclear periphery), CD56, Syn, CgA,

and CD117. Hepatic metastatic pulmonary adenocarcinoma must be differentiated from primary liver hepatocellular carcinoma and cholangiocarcinoma. These tumors lack specific morphological features and are primarily identified using immunohistochemistry. Metastatic pulmonary adenocarcinoma expresses markers of pulmonary adenocarcinoma, such as TTF-1 and Napsin A. Primary liver hepatocellular carcinoma expresses markers of the liver, such as HepPar-1, whereas cholangiocarcinoma expresses CK7 and CK19; neither of the latter expresses markers of pulmonary adenocarcinoma.

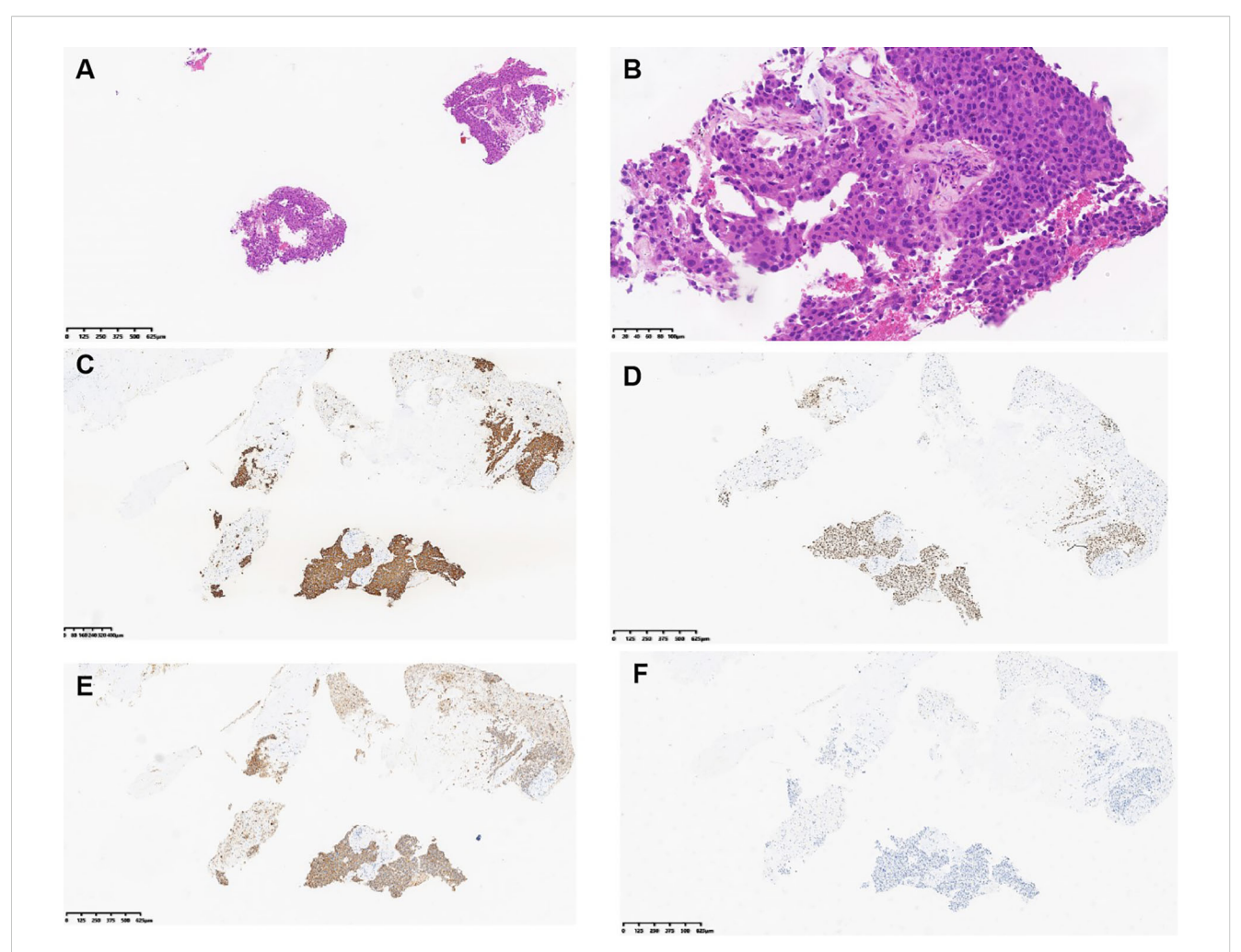
#### 3.3 Molecular features

The genetic variations in the two cases are shown in Table 1. In FISH, red-green separation and a single green signal were observed in more than 30% of the tumor cells, suggesting *NTRK2* gene rearrangement (Figures 4A, B).

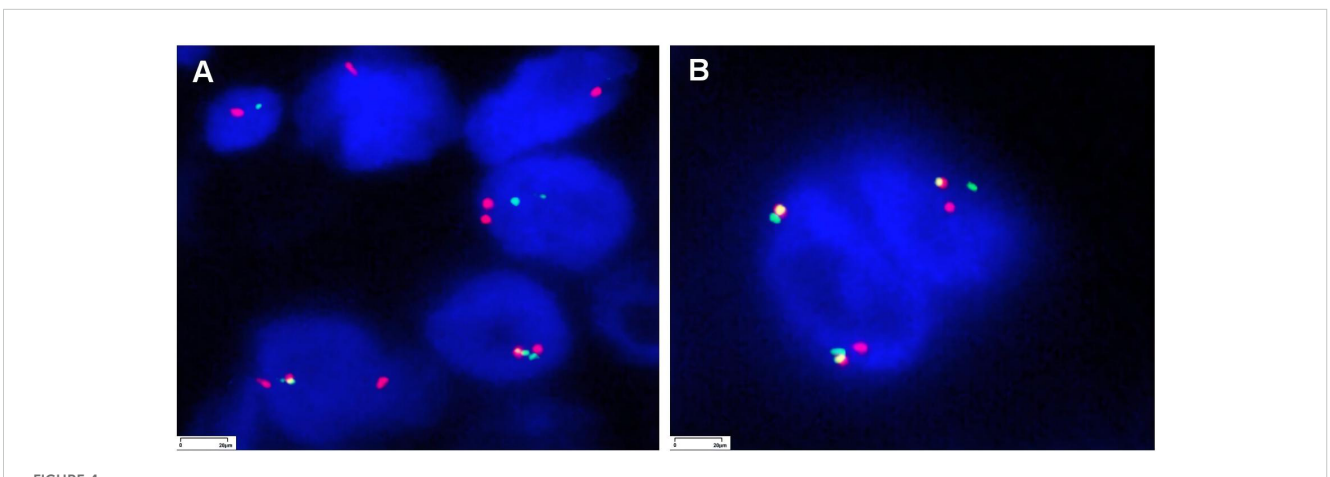
#### 3.4 Treatment and follow-up

#### 3.4.1 Patient 1

On November 10, 2022, and from November 11 to November 30, the patient underwent gamma knife treatment for intracranial metastases. The treatment process proceeded smoothly. A follow-up cranial CT scan showed partial shrinkage of the metastases and edema of the surrounding brain tissue. On November 11, 2022, the patient underwent the first cycle of pemetrexed and cisplatin chemotherapy. On November 16, 2022, the results of the primary lesion gene test indicated an EGFR exon 21 mutation, and the patient was administered osimertinib targeted therapy. During the treatment period, the patient did not experience any obvious discomfort and did not undergo regular follow-up. On May 1, 2023, follow-up lung CT showed a slightly smaller lesion area. On July 25, 2023, a follow-up cranial CT scan showed an increased lesion area. Subsequently, the patient underwent gamma knife treatment for the cranial metastases, and the treatment process was smooth. Simultaneously, a follow-up lung CT showed no significant changes in the lesion. Therefore, from



Hematoxylin and eosin (H&E) and immunohistochemical images of the liver lesion biopsy of patient 1. (A) H&E staining, magnification ×40. (B) H&E staining, magnification ×200. (C) Tumor expressed CK7. (D) Tumor expressed TTF-1. (E) Tumor expressed Napsin (A). (F) Tumor did not express HepPar-1. (C-F) Magnification ×40.



Fluorescence in situ hybridization (FISH) images for NTRK testing of the liver tumor in patient 1 and lung tumor in patient 2 (magnification x1,000).

requency Copy number requency Variant Variant 78.35% 12.42% 18.28% 16.91 Variant region region Exon 9 /arian Exon 21 Exon 21 Amino acid substitution substitution Amino acid p.L858R p.L861Q p.H409Y GR (downstream KDM4C)~NTRK2 intron 14 (upstream DMAC1)~NTRK2 intron 14 17 GR (upstream CEP78)~NTRK2: exon Nucleotide Nucleotide alteration :.2573T>G c.2582T>A c.1225C>T Variant region Variant region Variant region 7q31.2 Type of gene Missense mutation Missense mutation Type of gene Missense mutation IGR ( variation variation Franscript NM\_005228.5 NM\_023110.3 Franscript NM 005228.5 number numbel Gene rearrangement /ariant genes /ariant genes Gene rearrangement Gene amplification FGFR1 NTRK2 EGFR MET MSI status MSS MSS TMB-L TMB TMB-L TMB 7.9 6.9 **Patients** Case 2 Case 1

Genetic variations of the two cases.

**FABLE 1** 

October 30, 2023, to January 17, 2024, the patient received four cycles of bevacizumab and sintilimab treatment and continued osimertinib maintenance therapy. The treatment process proceeded smoothly. The patient did not undergo regular follow-up. On April 4, 2024, a follow-up cranial CT scan showed no significant changes in the extent of metastasis. On September 24, 2024, a CT scan showed that the lung lesion had increased relative to previous imaging, and multiple lowdensity lesions appeared in the liver, which were considered metastases. A left adrenal adenoma was also considered a metastasis. A liver metastasis biopsy was performed on October 23, 2024, and genetic testing was conducted. On November 5, 2024, left adrenal secondary malignant tumor particle implantation treatment was performed, and the process was smooth. Because the genetic test of the liver metastasis revealed EGFR exon 21 mutation, NTRK2 gene fusion, MET amplification, and FGFR1 mutation, on November 25, 2024, the patient was treated with osimertinib combined with certolizumab until January 2025. For economic reasons, bozitinib was used. The patient did not undergo regular follow-up. During the follow-up period until June 2025, a total of 32 months, the patient's condition progressed slowly.

#### 3.4.2 Patient 2

Based on the genetic test results of the lung biopsy tissue, furmonertinib targeted therapy was initiated on May 9, 2024. The patient did not undergo regular follow-up. On November 11, 2024, CT reexamination showed that the lung lesion had improved. The patient was followed up until June 2025 for 13 months, and the condition was well-controlled.

#### 4 Discussion

The NTRK family consists of three members, NTRK1, NTRK2, and NTRK3, which are located at different segments of chromosomes 1q22, 9q21, and 15q25 and encode the tropomyosin-related kinase family proteins TRKA, TRKB, and TRKC, respectively. Fusions of NTRK1, NTRK2, and NTRK3 and their partner genes can lead to overexpression of Trk proteins, which in turn activate downstream signaling pathways, such as RAS/MAPK, PI3K/AKT, and PLC-γ, causing transformation, proliferation, and survival of cancer cells. NTRK fusion has been identified as a definite oncogenic driver (6) and is a valuable target for cancer treatment. The frequency of NTRK fusions in common solid tumors is extremely low, with a prevalence of 0.3 to 0.5% (7–9), including in NSCLC.

Recently, the prevalent methods for detecting NTRK fusions have included immunohistochemistry, FISH, reverse transcription polymerase chain reaction (PCR), and second-generation sequencing. However, each method has its own limitations. The European Society for Medical Oncology (6) recommended that FISH, reverse transcription PCR, or second-generation sequencing with RNA-based sequencing panels be used in tumors with frequent NTRK fusions, whereas for tumors with rare NTRK fusions, first-line sequencing (prioritizing RNA sequencing) or initial screening by immunohistochemistry should be performed for NTRK fusion-positive cases. RNA-based second-generation sequencing methods are considered the gold standard for all types of tumors (10, 11).

The most common fusions in solid tumors are ETV6:NTRK3 and TPM3:NTRK1 (12). More than 20 *NTRK1*, *NTRK2*, and *NTRK3* fusion partners have been identified in NSCLC (13), which usually do not coexist with other oncogenic drivers, such as *EGFR*, *ALK*, *ROS1*, *MET*, and *RET* (14). In the present study, *NTRK2* gene fusion was detected in two NSCLC cases, and the unique upstream region of the gene was the fusion location of the partner gene. The partner gene in Case 1 was located upstream of *CEP78*, and in Case 2, the fusion was located downstream of *KDM4C* and upstream of *DMAC1*. Notably, both mutations were accompanied by *EGFR* mutations (p.L858R and p.L861Q). The difference between the two cases was that a secondary *NTRK2* gene fusion was detected in the metastatic lesion in Case 1, whereas in Case 2, it was detected in a primary lung lesion.

A previous study (15) demonstrated that the emergence of *NTRK1* gene fusions may be a mechanism of resistance to epidermal growth factor receptor–tyrosine kinase inhibitors (EGFR-TKIs; such as osimertinib). The Guidelines for Clinical Practice of Molecular Tests in Non-Small Cell Lung Cancer in China (2024) stated that, in practical clinical settings, during the comprehensive analysis of acquired resistance to EGFR-TKIs, detection of NTRK fusion status is of particular importance (10). We did not observe *NTRK2* fusion in the primary lung lesion in Case 1. Instead, we detected *NTRK2* fusions in metastatic lesions after EGFR-TKI treatment (osimertinib). Therefore, we speculate that *NTRK2* fusion may also be a potential resistance mechanism to EGFR-TKIs. However, this conclusion should be verified by further studies with larger clinical sample sizes and basic research.

Currently, the targeted therapeutic drugs approved for NTRK fusion-positive solid tumors (16, 17) include larotrectinib, entrectinib, and repotrectinib. Repotrectinib is also used to treat adult patients with ROS1 fusion-positive locally advanced or metastatic NSCLC and patients with NTRK fusion-positive advanced solid tumors who have received one or two frontline tropomyosin receptor kinase (TRK) or TKI therapies without a satisfactory response or alternative options.

Interestingly, in Case 1, *MET* amplification and *FGFR1* mutations were also observed in the liver metastases. The proportion of primary *MET* gene amplification in NSCLC is 1%–5% (18), which is often secondary to targeted therapy in other driver gene-positive patients with NSCLC and is recognized as one of the important mechanisms related to EGFR-TKI resistance. *MET* amplification occurs in 7%–15% of patients with first-line EGFR-TKI drug resistance and in 5%–50% of patients with second-line EGFR-TKI drug resistance (19). In Case 1, osimertinib, a third-generation EGFR-TKI drug, was used, and *MET* amplification was observed in the secondary metastases, which may be a sign of osimertinib resistance. Therefore, the treatment strategy was changed to osimertinib combined with the MET amplification inhibitor (savolitinib), and the patient achieved a partial response.

FGFR1 is a member of the FGFR family, which mainly includes four subtypes. In solid tumors, the types of the FGFR1–4 genes vary. For example, amplification/overexpression is the most common variation in FGFR1, and fusion in FGFR2; single-nucleotide polymorphisms occur more frequently in both FGFR2 and FGFR3. Previous data showed that FGFR mutations occur more frequently in

Chinese than in Western populations, based on data from 10,194 Chinese patients with solid tumors (20), with gene amplification being the dominant form of variation (58.2%). The most common tumor types were urothelial neoplasms (30.5%) and endometrial carcinomas (16.9%). The *FGFR1* mutation (H409Y) in the liver metastases of Case 1 was a somatic mutation, which is a non-hotspot mutation recorded in the database. Although there is currently no clear clinical indication for targeted therapy, abnormal activation of FGFR in lung cancer remains noteworthy, as it may provide a beneficial treatment strategy.

Previous data published by Gatalica et al. (12) showed that PD-L1 expression was positive in 23% of NTRK fusion cancer cases. In the present study, PD-L1 expression was observed in two cases of *NTRK2* fusion. TMB and microsatellite status detected TMB-L and MSS in both cases, which were largely consistent with previous results (12).

The two patients reported in this article were treated with different EGFR tyrosine kinase inhibitors based on the results of genetic testing. After targeted therapy, the patients achieved varying degrees of remission. In Case 1, after disease progression, the gene test results of the metastatic tumors revealed MET gene amplification. This indicates that after developing resistance to EGFR-TKIs, the addition of a MET amplification inhibitor led to disease remission. In Cases 1 and 2, EGFR mutations and NTRK fusions occurred simultaneously. Although the frequency of both occurring simultaneously in patients with lung cancer is very low, targeting both EGFR and NTRK fusions together may provide clinical benefits (21), making them a treatment option for patients who have developed resistance to EGFR-TKIs. However, the treatment outcome depends on the specific resistance mechanism. Therefore, more cases need to be collected in the future to further study the efficacy and safety of combined treatment with EGFR-TKIs and NTRK inhibitors.

In conclusion, although NTRK fusions are rare in patients with NSCLC, the detection of NTRK fusions has gained importance with the development of TRK inhibitors. Therefore, we believe that NTRK fusions may represent a viable detection target or a target occurring simultaneously with other pathogenic and/or potentially targetable alterations, providing a promising opportunity for exploring combination therapies in future studies.

# Data availability statement

The datasets presented in this study can be found in online repositories. The names of the repository/repositories and accession number(s) can be found below: https://www.ncbi.nlm.nih.gov/, PRJNA1289990.

#### **Ethics statement**

The human-related research has been approved by the Ethics Committee of Weifang People's Hospital. These studies were conducted in accordance with local regulations and institutional requirements. For any images or data in this article that may identify individual identities, the relevant individuals (or their agents) have

given written informed consent for publication. Written informed consent was obtained from the participant/patient(s) for the publication of this case report.

#### **Author contributions**

YZ: Funding acquisition, Project administration, Validation, Writing – original draft, Writing – review & editing, Data curation, Formal Analysis, Investigation, Methodology, Visualization. HZ: Data curation, Writing – review & editing. XL: Funding acquisition, Project administration, Validation, Writing – original draft, Writing – review & editing, Conceptualization.

### **Funding**

The author(s) declare financial support was received for the research and/or publication of this article. The present study was funded by The Weifang Science and Technology Development Plan Project (grant number 2023YX013) and The Weifang Youth Medical Talent Lift Project.

# **Acknowledgments**

We would like to thank Editage (www.editage.cn) for English language editing.

#### Conflict of interest

The authors declare that the research was conducted in the absence of any commercial or financial relationships that could be construed as a potential conflict of interest.

#### References

- 1. Li W, Qiu T, Ling Y, Gao S, Ying J. Subjecting appropriate lung adenocarcinoma samples to next-generation sequencing-based molecular testing: challenges and possible solutions. *Mol Oncol.* (2018) 12:677–89. doi: 10.1002/1878-0261.12190
- 2. Si X, Pan R, Ma S, Li L, Liang L, Zhang P, et al. Genomic characteristics of driver genes in Chinese patients with non-small cell lung cancer. *Thorac Cancer.* (2021) 12:357–63. doi: 10.1111/1759-7714.13757
- 3. Chen J, Yang H, Teo ASM, Amer LB, Sherbaf FG, Tan CQ, et al. Genomic landscape of lung adenocarcinoma in East Asians. *Nat Genet.* (2020) 52:177–86. doi: 10.1038/s41588-019-0569-6
- 4. Gregg JP, Li T, Yoneda KY. Molecular testing strategies in non-small cell lung cancer: optimizing the diagnostic journey. *Transl Lung Cancer Res.* (2019) 8:286–301. doi: 10.21037/tlcr.2019.04.14
- 5. Robledano R, Lozano MD. An odd dancing couple. Non-small cell lung carcinoma with coexisting EGFR mutation and NTRK-1 translocation: A case report. *Diagn Cytopathol.* (2024) 52):393–6. doi: 10.1002/dc.25325
- 6. Marchiò C, Scaltriti M, Ladanyi M, Iafrate AJ, Bibeau F, Dietel M, et al. ESMO recommendations on the standard methods to detect NTRK fusions in daily practice and clinical research. *Ann Oncol.* (2019) 30:1417–27. doi: 10.1093/annonc/mdz204
- 7. Romanko AA, Mulkidjan RS, Tiurin VI, Saitova ES, Preobrazhenskaya EV, Krivosheyeva EA, et al. Cost-efficient detection of NTRK1/2/3 gene fusions: single-center analysis of 8075 tumor samples. *Int J Mol Sci.* (2023) 24):14203. doi: 10.3390/ijms241814203

#### Generative AI statement

The author(s) declare that no Generative AI was used in the creation of this manuscript.

Any alternative text (alt text) provided alongside figures in this article has been generated by Frontiers with the support of artificial intelligence and reasonable efforts have been made to ensure accuracy, including review by the authors wherever possible. If you identify any issues, please contact us.

#### Publisher's note

All claims expressed in this article are solely those of the authors and do not necessarily represent those of their affiliated organizations, or those of the publisher, the editors and the reviewers. Any product that may be evaluated in this article, or claim that may be made by its manufacturer, is not guaranteed or endorsed by the publisher.

# Supplementary material

The Supplementary Material for this article can be found online at: https://www.frontiersin.org/articles/10.3389/fonc.2025.1664782/full#supplementary-material

#### SUPPLEMENTARY FIGURE 1

Lung tumor hematoxylin and eosin staining of patient 1 (magnification,  $\times 200$ ).

#### SUPPLEMENTARY FIGURE 2

The Hematoxylin and eosin (HE) and immunohistochemical images of the lung tumor biopsy of patient 2. **(A)** HE staining, magnification, ×40; **(B)** HE staining, magnification, ×200; **(C)** Tumor expressed CK7; **(D)** Tumor expressed TTF-1; **(E)** Tumor did not expressed CK5/6; **(F)** Tumor did not expressed P40; **(C–F)** magnification, ×100.

- 8. Solomon JP, Linkov I, Rosado A, Mullaney K, Rosen EY, Frosina D, et al. NTRK fusion detection across multiple assays and 33,997 cases: diagnostic implications and pitfalls. *Mod Pathol.* (2020) 33:38–46. doi: 10.1038/s41379-019-0324-7
- 9. de Oliveira Cavagna R, de Andrade ES, Tadin Reis M, de Paula FE, Noriz Berardinelli G, Bonatelli M, et al. Detection of NTRK fusions by RNA-based nCounter is a feasible diagnostic methodology in a real-world scenario for non-small cell lung cancer assessment. *Sci Rep.* (2023) 13:21168. doi: 10.1038/s41598-023-48613-4
- 10. Pathology Quality Control Center, Chinese Society of Pathology, Chinese Medical Association Chinese Society of Oncology, China Anti-Cancer Association Chinese Society of Lung Cancer and Chinese Thoracic Oncology Group. Guidelines on clinical practice of molecular tests in non-small cell lung cancer in China (2024 version). Zhonghua Bing Li Xue Za Zhi. (2024) 53:981–95. doi: 10.3760/cma.j.cn112151-20240527-00338
- 11. Dong K, Zhu Y, Liu X, Sun W, Yang X, Chi K, et al. Feasibility of two-step approach for screening NTRK fusion in two major subtypes of non-small cell lung cancer within a large cohort. *Hum Pathol.* (2024) 149:39–47. doi: 10.1016/j.humpath.2024.06.003
- 12. Gatalica Z, Xiu J, Swensen J, Vranic S. Molecular characterization of cancers with NTRK gene fusions. *Mod Pathol.* (2019) 32:147–53. doi: 10.1038/s41379-018-0118-3
- 13. Overbeck TR, Reiffert A, Schmitz K, Rittmeyer A, Körber W, Hugo S, et al. NTRK gene fusions in non-small-cell lung cancer: real-world screening data of 1068 unselected patients. *Cancers (Basel)*. (2023) 15:2966. doi: 10.3390/cancers15112966

- 14. Haratake N, Seto T. NTRK fusion-positive non-small-cell lung cancer: the diagnosis and targeted therapy. *Clin Lung Cancer*. (2021) 22:1–5. doi: 10.1016/j.cllc.2020.10.013
- 15. Xia H, Xue X, Ding H, Ou Q, Wu X, Nagasaka M, et al. Evidence of NTRK1 fusion as resistance mechanism to EGFR TKI in EGFR+ NSCLC: results from a large-scale survey of NTRK1 fusions in chinese patients with lung cancer. *Clin Lung Cancer*. (2020) 21:247–54. doi: 10.1016/j.cllc.2019.09.004
- 16. Russo A, Lopes AR, McCusker MG, Garrigues SG, Ricciardi GR, Arensmeyer KE, et al. New targets in lung cancer (Excluding EGFR, ALK, ROS1). *Curr Oncol Rep.* (2020) 22):48. doi: 10.1007/s11912-020-00909-8
- 17. Farago AF, Taylor MS, Doebele RC, Zhu VW, Kummar S, Spira AI, et al. Clinicopathologic features of non-small-cell lung cancer harboring an NTRK gene fusion. *JCO Precis Oncol.* (2018) 2:1-12. doi: 10.1200/PO.18.00037
- 18. Guo R, Luo J, Chang J, Rekhtman N, Arcila M, Drilon A. MET-dependent solid tumours molecular diagnosis and targeted therapy. *Nat Rev Clin Oncol.* (2020) 17:569–87. doi: 10.1038/s41571-020-0377-z
- 19. Leonetti A, Sharma S, Minari R, Perego P, Giovannetti E, Tiseo M. Resistance mechanisms to osimertinib in EGFR-mutated non-small cell lung cancer. *Br J Cancer*. (2019) 121:725–37. doi: 10.1038/s41416-019-0573-8
- 20. Wu L, Yao H, Chen H, Wang A, Guo K, Gou W, et al. Landscape of somatic alterations in large-scale solid tumors from an Asian population. *Nat Commun.* (2022) 23:4264. doi: 10.1038/s41467-022-31780-9
- 21. Wang JL, Wang LS, Zhu JQ, Ren J, Wang D, Luo M. Survival benefit of combinatorial osimertinib rechallenge and entrectinib in an EGFR-mutant NSCLC patient with acquired LMNA-NTRK1 fusion following osimertinib resistance. *Respirol Case Rep.* (2022) 10:e01054. doi: 10.1002/rcr2.1054